



Projected decrease in wintertime bearing capacity on different forest and soil types in Finland under a warming climate

Ilari Lehtonen¹, Ari Venäläinen¹, Matti Kämäräinen¹, Antti Asikainen², Juha Laitila², Perttu Anttila² and Heli Peltola³

5 ¹Finnish Meteorological Institute, 00101 Helsinki, Finland

²Natural Resources Institute Finland, 80100 Joensuu, Finland

³School of Forest Sciences, University of Eastern Finland, 80101 Joensuu, Finland

Correspondence to: Ilari Lehtonen (ilari.lehtonen@fmi.fi)

Abstract. Trafficability in forest terrain is largely determined by ground-bearing capacity and it is thus one of the most 10 important issues in timber harvesting. In winter, the bearing capacity is mainly determined by soil frost. Particularly on peatland forests bearing capacity is poor under unfrozen conditions. The bearing capacity of forest truck roads is similarly affected by ground frost. Already 20 cm thick layer of frozen soil or 40 cm layer of snow on the ground can carry in Finnish forest conditions heavy machines in forest harvesting. In this work, we studied the impacts of climate change on soil frost conditions, and consequently on ground-bearing capacity of soils from the timber harvesting point of view. The number of days with good 15 wintertime bearing capacity was modelled by using a soil temperature model and wide set of downscaled climate model data until the end of the 21st century. The model was optimized for different forest and soil types. The results show that by the mid-21st century, the wintertime bearing season length decreases in Finland most likely by about one month. The decrease in soil frost and wintertime bearing capacity will be more pronounced during the latter half of the century when drained peatlands may virtually lack soil frost in most of winters in southern and western Finland. The projected decrease in the bearing capacity, 20 accompanied with increasing demand for wood harvesting from drained peatlands, induces a clear need for the development of new sustainable and efficient logging practices for drained peatlands.

1 Introduction

During 2004–2013, the annual harvested volume of round wood in Finland was on average 60 mill. m³ (Finnish Forest Research Institute, 2014) of which most was consumed in the chemical pulp industry and sawmilling industry (Natural 25 Resources Institute Finland, 2017a). The national strategy for bioeconomy in Finland targets to increase the economic output of entire bioeconomy sector from €63 billion in 2014 to €100 billion by 2020 (Ministry of Employment and the Economy et al., 2014; Asikainen et al., 2016). This relies largely on the increasing use of the abundant forest resources in the country. To meet the wood demand of the growing bioeconomy sector, there is a pressure to increase the annual wood harvesting of Finnish forests up to 80 mill. m³ within the next couple of decades (Ministry of Employment and the Economy et al., 2014). Already 30 in 2016, the annual harvested volume of round wood reached a new national record of 70 mill. m³ (Natural Resources Institute



Finland, 2017b). Preferably the wood harvesting should be increased throughout the year to reduce the adverse impacts of seasonal variation of harvesting on the capacity utilization of harvesting and transport fleet. This may be challenging due to differences in bearing capacity of forest soils with varying soil types and weather conditions.

5 In Finland, timber harvesting is based on the cut-to-length method (Nurminen et al., 2006; Nurminen and Heinonen, 2007; Manner et al., 2017). Fully mechanized modern cut-to-length logging system consists of harvester and forwarder. A harvester cuts and delimbs the trees and crosscuts the stems into assortments. The logs are then transported to roadside landings for temporary storing by a forwarder. The final transport to the end-users is usually carried out by heavy timber trucks (Nurminen and Heinonen, 2007; Malinen et al., 2014; Wolfsmayr and Rauch, 2014). The functionality of wood supply chain is a crucial
10 issue because the demand of raw material is constant throughout the year and the volumes of timber harvest and transportation are great. However, traditionally logging has been mainly conducted during winter months. Still nowadays, approximately 60% of logging is carried out while the soil is frozen, between October and March (Finnish Forest Research Institute, 2014). It is because in the case of frozen soil, the bearing capacity of forest sites is clearly higher than in unfrozen soil conditions. Already 20 cm thick layer of frozen soil or 40 cm thick layer of snow can bear standard machines used in forest harvesting
15 that weigh 15–30 tonnes (Eeronheimo, 1991). Small forest truck roads having light foundations do not either bear heavy timber trucks in wet road sections unless the soil is frozen (Kaakkurivaara et al., 2015). Multiple passes of a harvester and a loaded forwarder may cause ruts on the forest floor (Suvinen, 2006; Sirén et al., 2013; Pohjankukka et al., 2016). Operations in poorly bearing conditions increase this rut formation and damage caused to tree roots and stems as well as time and fuel consumption in the harvesting (Sirén et al., 2013; Pohjankukka et al., 2016). Furthermore, the condition of road network affects to the fuel
20 consumption in timber transportation (Svenson and Fjeld, 2016).

More than half of the original peat bog area in Finland was drained for forestry mainly during the 1960s and 1970s (Simola et al., 2012). Consequently, peatlands consist nowadays one third of the Finnish forestry area and one fourth of the growing stock volume (Ala-Ilomäki et al., 2011). In increasing the wood harvesting, more intensive utilization of drained peatland forests has the largest potential (Ala-Ilomäki et al., 2011), because of a pronounced reduction of suitable logging sites
25 on upland (mineral) soils (Uusitalo and Ala-Ilomäki, 2013). However, more intensive utilization of peatlands is a controversial issue. Peatlands representing sensitive forest sites are generally characterized by the most difficult forest harvesting conditions (Nugent et al., 2003; Uusitalo and Ala-Ilomäki, 2013; Uusitalo et al., 2015a). Moreover, in addition to the increasing demand of wood harvesting from drained peatlands, there exists a pressure to restore drained peatlands to natural state in order to maintain biodiversity and prevent carbon loss from peatlands (Komulainen et al., 1999; Carroll et al., 2011; Pitkänen et al.,
30 2013).

The difficult harvesting conditions in drained peatlands are because of their inherently low ground-bearing capacity. Thus, logging is there generally conducted during winter when the soil is frozen (Ala-Ilomäki et al., 2011). Nevertheless, soil frost periods are on drained peatlands shorter than on upland forest sites because of the insulating effect of peat compared to upland (mineral) soils. In addition, ditch network forms obstacles for vehicles in peatlands. They are neither typically located



next to the forest truck roads and trees are characterized by small size, uneven distribution and superficial roots (Laitila et al., 2013). Hence, wood harvesting on drained peatlands is in general less cost efficient than in upland forest sites (Ala-Ilomäki et al., 2011). Determined efforts are thus required to prolong the wood harvesting season from drained peatlands. This would provide an opportunity to increase the annual harvesting volume and confine seasonal variations in harvesting.

5 During the forthcoming decades, climate has been projected to become warmer due to the anthropogenic climate change (Collins et al., 2013; Knutti and Sedláček, 2013). The climate warming is expected to be pronounced on high latitudes like in Finland (Räisänen and Ylhäisi, 2015; Ruosteenoja et al., 2016). Previous studies have indicated that the climate warming leads unsurprisingly to reduced soil frost depth and shorter soil frost periods (Venäläinen et al., 2001a, 2001b; Kellomäki et al., 2010; Jungqvist et al., 2014). This may shorten the winter harvesting season with good ground-bearing capacity, 10 particularly on drained peatlands, having thus mainly negative impact on the forestry sector. Thus, comprehensive understanding of expected changes in soil frost conditions is utmost important as these changes affect wood harvesting conditions and transport availability. This is also needed to develop logging practices that are at the same time both sustainable and cost-efficient and meet the required bioeconomy and climate change mitigation goals.

There are several models designed for calculation of soil temperatures (e.g., Yin and Arp, 1993; Rankinen et al., 2004; 15 Jansson, 2012; Park et al., 2017). In principle, the models approximate the solutions of differential equations describing water and heat flow. In conjunction with climate model data, these models can be utilized in evaluating the climate change impacts on soil temperature and frost conditions (e.g., Sinha and Cherkauer, 2010; Houle et al., 2012; Jungqvist et al., 2014; Oni et al., 2017). In this study, we used a relatively simple soil temperature model developed originally by Rankinen et al. (2004). The 20 only meteorological variables needed in the model calculations were daily mean air temperature and snow depth. Our objective was to study the impacts of projected climate warming by 2100 on soil frost conditions, and consequently, on bearing capacity of different forest and soil types in Finland with regard to wintertime wood harvesting conditions and transport availability on forest truck roads. We used the soil temperature model in evaluating the soil frost conditions which largely define the ground-bearing capacity in winter. The ground-bearing capacity was assumed to be good if the depth of soil frost was at least 20 cm or depth of snow cover was at least 40 cm. First, we optimized the model parameters, by describing, e.g. soil thermal 25 conductivity and specific heat capacity of soil for different soil types based on soil temperature observations from several stations across Finland. The effect of forest density on snow cover was also taken into account. Then, we evaluated the wintertime bearing capacity in future climatic conditions by using daily data from several global and regional climate model simulations downscaled onto an approximately 10 km × 10 km grid. The used global climate model (GCM) data were extracted from the Coupled Model Intercomparison Project phase 5 (CMIP5) database (Taylor et al., 2012) while the used regional 30 climate model (RCM) simulations were constructed within the EURO-CORDEX project (Jacob et al., 2014). The climate simulations were extended until 2099, considering two representative concentration pathway (RCP) scenarios, RCP4.5 and RCP8.5 (van Vuuren et al., 2011). We used data from wide set of climate models under the two emission scenarios to achieve a comprehensive picture of possible future outcomes. To foster the use of our results in forestry applications, the data describing the bearing capacity in different forest stands over different periods will also be made publicly available.



2 Material and methods

2.1 Outlines for soil temperature model and its parametrization and validity

2.1.1 Outlines for soil temperature model

Soil temperatures were calculated by using an extended version of soil temperature model originally introduced by Rankinen et al. (2004). The model is derived from the law of conservation of energy and mass assuming constant water content in the soil. According to the model, soil temperature at depth Z_S can be calculated as follows:

$$T_Z^{t+1} = T_Z^t + \frac{\Delta t \cdot K_T}{C_A \cdot (2 \cdot Z_S)^2} \cdot [T_{AIR}^t - T_Z^t], \quad (1)$$

where T_Z^t ($^{\circ}\text{C}$) is the soil temperature on a previous day, T_{AIR} ($^{\circ}\text{C}$) is the air temperature, Δt is the length of a time step (s), K_T ($\text{W m}^{-1} \text{ }^{\circ}\text{C}^{-1}$) is the thermal conductivity of the soil and C_A ($\text{J m}^{-3} \text{ }^{\circ}\text{C}^{-1}$) is the heat capacity of the soil. C_A can be approximated as follows:

$$C_A \approx C_S + C_{ICE}, \quad (2)$$

where C_S ($\text{J m}^{-3} \text{ }^{\circ}\text{C}^{-1}$) is the specific heat capacity of the soil and C_{ICE} ($\text{J m}^{-3} \text{ }^{\circ}\text{C}^{-1}$) is the specific heat capacity due to freezing and thawing. When $T_Z^t > 0 \text{ }^{\circ}\text{C}$, the latter term equals to 0.

As Eq. (1) did not take the insulating effect of snow cover into account, the equation was extended by an empirical relationship (Rankinen et al., 2004):

$$T_Z^{t+1} = T_Z^t + \frac{\Delta t \cdot K_T}{(C_S + C_{ICE}) \cdot (2 \cdot Z_S)^2} \cdot [T_{AIR}^t - T_Z^t] \cdot [e^{-f_S \cdot D_S}], \quad (3)$$

where f_S (m^{-1}) is an empirical damping parameter and D_S (m) is snow depth. This model assumed that there is no heat flow below the soil layer of consideration. To extend the model, Jungqvist et al. (2014) added parameters controlling the lower soil thermal conductivity $K_{T,LOW}$ ($\text{W m}^{-1} \text{ }^{\circ}\text{C}^{-1}$), lower soil specific heat capacity $C_{S,LOW}$ ($\text{J m}^{-3} \text{ }^{\circ}\text{C}^{-1}$), and lower soil temperature T_{LOW} ($^{\circ}\text{C}$):

$$T_Z^{t+1} = T_Z^t + \frac{\Delta t \cdot K_T}{(C_S + C_{ICE}) \cdot (2 \cdot Z_S)^2} \cdot [T_{AIR}^t - T_Z^t] \cdot [e^{-f_S \cdot D_S}] + \frac{\Delta t \cdot K_{T,LOW}}{(C_{S,LOW} + C_{ICE}) \cdot (2 \cdot (Z_l - Z_S))^2} \cdot [T_{LOW} - T_Z^t], \quad (4)$$

where Z_l (m) is the depth where T_{LOW} prevails.

We assumed T_{LOW} to be equal to the mean 2-m air temperature of previous 365 days and the values of parameters K_T , C_S , C_{ICE} , f_S , $K_{T,LOW}$, $C_{S,LOW}$ and Z_l were optimized based on soil temperature observations. According to Eeronheimo (1991), 20 cm thick layer of frozen soil or 40 cm thick snow cover makes the terrain passable for heavy harvesters even in soil types characterized by low bearing capacity. Keeping this in mind, the emphasis in optimizing the parameters was given near the surface. Moreover, the parameters controlling heat flow below the soil layer under consideration had only negligible effect on modelled soil temperatures near the surface.



2.1.2 Parametrization of soil temperature model

In the optimization of the parameters, we used soil temperature observations from the stations listed in Table 1. The model was allowed to spin up for 1 year to reach thermal equilibrium in all of our calculations. Soil temperatures were measured every fifth day, except from Lettosuo, Apukka, Lompolojänkkä and Kaamanen the measurements were available on a daily basis. However, there were some time periods with missing data at these sites. The stations represented different soil types. The soil types were extracted from Soveri and Varjo (1977) and Heikinheimo and Fougstedt (1992), except for Lettosuo, Apukka, Lompolojänkkä and Kaamanen stations. According to the soil type map provided by the Geological Survey of Finland, the soil type at Apukka station is till. The Lettosuo station is situated in a drained peat bog and the stations Lompolojänkkä and Kaamanen are located on open fens. Snow depth measurements needed in the calculations were not available from Lettosuo, Lompolojänkkä and Kaamanen stations and at these sites, snow depths measured on nearby stations were used in the model optimization. Daily mean temperatures used in the model optimization were extracted from a gridded data set covering Finland (Aalto et al., 2016).

The optimal parameter values were set to each station and each available measurement depth. First, the soil temperature model was run 10 000 times, sampling a new set of randomized parameters for each run from the chosen parameter ranges (Table 2). The sampling ranges were adopted from Jungqvist et al. (2014) but for K_T the upper limit was extended from $1 \text{ W m}^{-1} \text{ K}^{-1}$ to $2 \text{ W m}^{-1} \text{ K}^{-1}$. Then, the set of parameters indicating the highest linear correlation between the observed and modelled soil temperatures at each station and each measurement depth was selected. For some parameters optimized values varied rather randomly within the sampling range between different depths and locations while, for example, K_T seemed to steadily increase with soil depth. After the first optimization round, Z_l was set to 6.8 m and f_s to 9.0 at each location and depth. Then, the soil temperature model was run additional 100 000 times with the fixed Z_l and f_s values while the other parameters were sampled again. After this second optimization round, all other parameters except K_T were also set to their final values. $K_{T,LOW}$ and $C_{S,LOW}$ were given the same values at all depths and locations while C_{ICE} was set to depend on the soil type and C_s the depth following asymmetrical sigmoid function. After that, the soil temperature model was run once more 10 000 times to sample only the K_T values. The optimized K_T values tended to increase with soil depth at each location (Fig. 1). Anjala, Sodankylä and Lettosuo stations were selected to represent clay/silt, sand and peat soil types, respectively. K_T for these soil types was then estimated by fitting a logistic regression curve on the optimized values on these locations (Fig. 1). In addition to clay/silt, sand and peat soils, we modelled the soil frost in forest truck roads. In this case, we assumed that there is no snow on the surface and the coefficients describing soil properties were set by giving 1/3 weight for the coefficients used to describe sand and 2/3 for those describing clay/silt. Final parameters used in the soil temperature calculations are listed in Table 3.

2.1.3 Validity of the modelled soil temperatures

Apart from the stations used in calibration of K_T for different soil types (Lettosuo, Anjala and Sodankylä), the modelled soil temperatures for clay/silt and sand soil types typically explained 90–99% of the observed variability in soil temperatures



between the depths of 20 and 100 cm (Table S1). Near the surface the modelled temperatures correlated slightly worse with the observed ones, as well as below 1 m. In spite of the generally high correlations, the modelled number of days with soil temperatures below 0 °C were still greatly overestimated (not shown). We also tested setting the model parameters by optimizing the modelled number of days with soil temperatures below 0 °C but then the correlations between observed and modelled soil temperatures became dramatically worse. In order to estimate more realistically the number of days with frozen soil, we thus assumed that the soil does not freeze until the soil temperature drops below –0.1 °C in sand or below –0.5 °C in other soil types. This was based on a study by Soveri and Varjo (1977) who stated that the freezing point in saturated sandy soil lies between 0 and –0.15 °C and in thin clay around –0.5 °C. Based on their study, in thick clay the freezing point can be as low as –20 °C, because the finer soil texture is, the stronger absorption and capillary water bound around the soil particles by reducing the freezing point. The melting point of soil was still set to 0 °C in all of our calculations.

2.2 Outlines for snow model and its parametrization and validity

2.2.1 Outlines for snow model

In order to estimate snow depth D_s needed in the soil temperature calculations, we used a temperature index snow model based largely on Vehviläinen (1992). Meteorological variables needed in the snow depth calculations are daily mean air temperature and daily total precipitation sum. First, the precipitation is divided into liquid and solid forms of precipitation as follows (Hankimo, 1976):

$$P_{solid} = P_{tot}, \text{ when } T_{mean} \leq -2.0 \text{ °C}$$

$$P_{solid} = \left(\frac{-T_{mean}}{8} + \frac{3}{4} \right) \cdot P_{tot}, \text{ when } -2.0 \text{ °C} < T_{mean} \leq 0.0 \text{ °C}$$

$$P_{solid} = \left(\frac{-25T_{mean}}{90} + \frac{3}{4} \right) \cdot P_{tot}, \text{ when } 0.0 \text{ °C} < T_{mean} \leq 0.9 \text{ °C}$$

$$P_{solid} = \left(\frac{-5T_{mean}}{8} + \frac{17}{16} \right) \cdot P_{tot}, \text{ when } 0.9 \text{ °C} < T_{mean} \leq 1.3 \text{ °C} \quad (5)$$

$$P_{solid} = \left(\frac{-T_{mean}}{8} + \frac{33}{80} \right) \cdot P_{tot}, \text{ when } 1.3 \text{ °C} < T_{mean} \leq 3.3 \text{ °C}$$

$$P_{solid} = 0, \text{ when } T_{mean} > 3.3 \text{ °C}$$

$$P_{liquid} = P_{tot} - P_{solid}$$

where P_{solid} (mm) is the amount of solid precipitation, P_{liquid} (mm) is the amount of liquid precipitation, P_{tot} (mm) is the total amount of precipitation and T_{mean} (°C) is the 2-metre daily mean air temperature.

The used snow model calculates the snow water equivalent (SWE) and density of snowpack. SWE (mm) is divided into two components as follows:

$$\text{SWE} = \text{SWE}_{new} + \text{SWE}_{old} \quad (6)$$

where SWE_{new} (mm) is the amount of SWE accumulated on the day considered and SWE_{old} (mm) describes the amount of snowpack left from the previous day. SWE_{new} is calculated as follows:

$$\text{SWE}_{new} = \text{cps} \cdot P_{solid} + \text{SWE}_{inc,liq} \quad (7)$$



where cps is a correction factor for solid precipitation and $SWE_{inc,liq}$ (mm) is the increase of water storage in snowpack due to liquid precipitation. $SWE_{inc,liq}$ is limited by the water retention capacity of snowpack (WH) which is proportional to the total amount of snowpack and is thus determined as follows:

$$WH = a \cdot SWE_{old} \quad (8)$$

5 where a is an empirical coefficient. $SWE_{inc,liq}$ is furthermore defined as follows:

$$SWE_{inc,liq} = P_{liquid}, \text{ when } P_{liquid} \leq WH$$

$$SWE_{inc,liq} = WH, \text{ when } P_{liquid} > WH \quad (9)$$

Decrease of SWE is caused both by evaporation from snowpack and by melting. Snowmelt is caused by thaw and liquid precipitation. Rainfall affects snowmelt directly by heating snowpack but more importantly, also by creating drains in the 10 snowpack and accelerating the ripening process of snow cover. SWE_{old} is then calculated as follows:

$$SWE_{old}^{t+1} = SWE_{old}^t + SWE_{new}^t - [km_t \cdot (T_{mean}^t - tm) - pm \cdot P_{liquid}^t \cdot (T_{mean}^t - tm) - ev] \cdot \Delta t \quad (10)$$

where km ($\text{mm} \text{ } ^\circ\text{C}^{-1} \text{ d}^{-1}$) is a degree-day factor, tm ($^\circ\text{C}$) is threshold air temperature for snowmelt, pm ($^\circ\text{C}^{-1} \text{ d}^{-1}$) is a melt factor related to liquid precipitation and ev ($\text{mm} \text{ d}^{-1}$) is evaporation from snowpack. The degree-day factor km is calculated as follows (Anderson, 1973):

$$15 \quad km = \frac{kmax + kmin}{2} + \sin\left(\frac{2N \cdot \Pi}{366}\right) \cdot (kmax - kmin) \quad (11)$$

where $kmax$ ($\text{mm} \text{ } ^\circ\text{C}^{-1} \text{ d}^{-1}$) is the degree-day factor on June 21st, $kmin$ ($\text{mm} \text{ } ^\circ\text{C}^{-1} \text{ d}^{-1}$) is the degree-day factor on December 21st and N is the day number beginning with March 21st.

Density of snow is calculated separately for new and old snow. Density of freshly fallen snow ($\rho_{s,new}$) is calculated as follows:

$$20 \quad \rho_{s,new} = b \cdot T_{mean} + c, \text{ when } \rho_{s,new} \geq \rho_{s,new,min} \quad (12)$$

where b ($\text{kg} \text{ m}^{-3} \text{ } ^\circ\text{C}^{-1}$) and c ($\text{kg} \text{ m}^{-3}$) are empirical coefficients and $\rho_{s,new,min}$ ($\text{kg} \text{ m}^{-3}$) is the minimum possible density of freshly fallen snow.

Density of old snow ($\rho_{s,old}$) is increased due to aging, thawing and liquid precipitation and is thus calculated as follows:

$$\rho_{s,old}^t = \rho_{s,old}^{t-1} + (\rho_{s,inc} + \rho_{s,inc,rain} \cdot P_{liquid}) \cdot \Delta t, \text{ when } \rho_{s,old}^t \leq \rho_{s,max} \quad (13)$$

25 where $\rho_{s,old}^{t-1}$ ($\text{kg} \text{ m}^{-3}$) is the density of snowpack on a previous day, $\rho_{s,inc}$ ($\text{kg} \text{ m}^{-3} \text{ d}^{-1}$) is the density increment due to aging and thawing of snowpack, $\rho_{s,inc,rain}$ ($\text{kg} \text{ m}^{-3} \text{ mm}^{-1} \text{ d}^{-1}$) is the density increment due to liquid precipitation and $\rho_{s,max}$ ($\text{kg} \text{ m}^{-3}$) is the maximum possible density of snowpack. $\rho_{s,inc}$ ($\text{kg} \text{ m}^{-3} \text{ d}^{-1}$) is defined as follows:

$$\rho_{s,inc} = \rho_{s,inc,age}, \text{ when } T_{mean} \leq 0 \text{ } ^\circ\text{C}$$

$$\rho_{s,inc} = \rho_{s,inc,age} + \rho_{s,inc,thaw} \cdot T_{mean}, \text{ when } T_{mean} > 0 \text{ } ^\circ\text{C} \quad (14)$$

30 where $\rho_{s,inc,age}$ ($\text{kg} \text{ m}^{-3} \text{ d}^{-1}$) is a coefficient defining the density increment of snowpack due to aging and $\rho_{s,inc,thaw}$ ($\text{kg} \text{ m}^{-3} \text{ } ^\circ\text{C}^{-1} \text{ d}^{-1}$) is a coefficient related to the density increment of snowpack due to thawing.

Finally, D_s (m) is calculated as follows:



$$D_S = \frac{SWE_{new}}{\rho_{S,new}} + \frac{SWE_{old}}{\rho_{S,old}} \quad (15)$$

2.2.2 Parametrization of snow model

Parameters for the snow model were optimized with a similar manner as for the soil temperature model. We randomly sampled 10 000 times the parameters a , b , c , cps, tm, pm, ev, kmax, kmin, $\rho_{s,new,min}$, $\rho_{s,max}$, $\rho_{s,inc,rain}$, $\rho_{s,inc,age}$ and $\rho_{s,inc,thaw}$ from the parameter ranges shown in Table 4. Then, the model was ran with each of these 10 000 set of parameters for the seven stations with soil temperature observations covering the period 2007–2014 (Table 1). The snow model was run over the period 1961–2014 by using the Finnish gridded climate data (Aalto et al., 2016) and the period 2006–2014 was used as the calibration period for the snow model. We minimized the root-mean-square error (RMSE) between modelled and observed snow depths on the stations during the calibration period by selecting the set of parameters indicating the smallest RMSE on each station. Then, the optimized parameters were averaged among all the seven stations to give the final parameters for the snow model (Table 5). Exceptions were kmax and kmin which seemed to show a latitudinal dependence as expected. These parameters were thus approximated by latitudinal-dependent exponent functions.

During the calibration period 2006–2014, the snow model with optimized parameters shown in Table 5 explained 94–96% of the observed variability in snow depth except at Apukka, where R^2 -value was only 0.84 (Table 5). When using the parameters optimized for each station before averaging, the R^2 -values were on average approximately 0.01 higher (not shown). We also tested the model with fixed kmax and kmin values averaged similarly as the other parameters and then the R^2 -values were on average 0.003 lower than those showed in Table 5. Except at Apukka, the model performance was in this case slightly worsen at every station.

As the snow depth measurement sites are located on open environments, the optimized parameters shown in Table 5 were used to model snow depth on open habitats. In forested areas, snow cover is reduced due to interception by the canopy, evaporation of the intercepted snow and enhanced wintertime snowmelt below the canopy (Hedstrom and Pomeroy, 1998; Varhola et al., 2010). Interception typically increases with increasing forest density and leaf area index (Lundberg and Koivusalo, 2003; Rasmus et al., 2013). Interception can be as high as nearly 50% of precipitation (Stähli and Gustafsson, 2006). In order to model the soil frost in different kind of forest stands, we added an interception coefficient to the snow model. In addition to open habitats, the calculations were performed for forests with three different density classes corresponding roughly to deciduous forest or sparse mixed forest, pine forest and dense spruce forest. The interception coefficients for these forest stands were extracted from Lundberg and Koivusalo (2003). To reduce the modelled snow cover in forests, SWE_{new} was multiplied with the interception coefficient in every time step.

Forest canopy also shelters snow cover from direct sunlight which reduces the degree-day factor. Vehviläinen (1992) presented experimental degree-day factors for open and forested areas for different river catchments and also based on earlier studies for both open areas and for different kind of forests (Gurevich, 1950; Hiitiö, 1982). Hence, we estimated the effect of forest density on degree-day factor based on Vehviläinen (1992). As it is moreover clear that the difference in degree-day



factor between open and forested areas is larger in summer than in winter, we reduced k_{max} more than k_{min} in forest environments. We moreover required that k_{max} cannot be smaller than k_{min} by setting k_{min} equal to k_{max} to indicate no annual course in degree-day factor in the case this would have otherwise happened. The coefficients used in reducing k_{max} and k_{min} as well as the interception coefficients used in this study for different forest types are shown in Table 5.

5 2.2.3 Validity of the modelled snow depths

The validation period 1962–2005 was divided into two sub-periods, 1962–1980 and 1981–2005, because the precipitation gauges and their wind shields in Finland were changed during 1981–1982 in order to improve catch efficiency of snow. Before 1981, Nipher-shielded Wild gauges were used and after 1982 shielded Tretyakov gauges which are known to suffer less from wind-induced undercatch of snowfall (Yang et al., 1999). During the period 1981–2005, the R^2 -values varied between 0.87 and 0.93, so the model performance was somewhat lower than during the calibration period. Before 1981, the model performance was even worse except at Apukka where the snow model performed best during the validation periods. This is probably related to the fact that the modelled snow depths in a grid cell surrounding the Apukka station were on average 31% higher than the observed ones at the station during the calibration period while at other stations the modelled and observed snow depths resembled each other more closely (Table S2). The overestimation of snow depth at Apukka might be related to local microclimatological characteristics as we used the gridded climate data in snow modelling, not the station observations. Already at Rovaniemi Airport weather station, located only at a distance of 7.9 km from the Apukka station, the observed snow depths tend to be remarkable higher (not shown). It is moreover noteworthy that modelled snow depths were in general systematically underestimated during the validation periods, especially before 1981. This indicates that a higher correction factor c_{ps} should have been used for the previous decades to improve the model performance.

20 2.3 Simulation of soil frost and snow depth for different forest and soil types under changing climatic conditions

The soil frost and snow depth calculations were performed for each possible combinations of three soil types and four forest types to evaluate the changes in soil bearing capacity. In addition, the calculations were performed for forest truck roads without snow cover leading to a total of 13 different combinations of soil and forest types. Calculations for each of these soil and forest types were performed on every grid cell. The simulation results were analysed for the near-future period 2021–2050 and for the far-future period 2070–2099 as compared to the baseline period 1981–2010. In addition, over the baseline period the soil temperature and snow depth models were ran also by using the observational Finnish gridded climate data (Aalto et al., 2016). We modelled the number of days with good bearing capacity in the forest harvesting point of view. Good bearing capacity was assumed to prevail when the soil frost penetrated continuously from the surface to at least the depth of 20 cm or when the snow depth exceeded 40 cm.

30 The calculations for the period 1980–2099 under changing climate were completed using daily data from six global climate models (Table S3) participating in the CMIP5 (Taylor et al., 2012; Flato et al., 2013), as bias-corrected and downscaled onto the Finnish grid. In addition, we used daily data from 11 bias-adjusted regional climate model (RCM) simulations (Table



S4) constructed within the EURO-CORDEX project (Jacob et al., 2014). Both were based on the RCP4.5 and RCP8.5 scenarios (van Vuuren et al., 2011), which are widely used in climate change impact studies. The RCP4.5 scenario represents a world characterized by relatively well succeeded mitigation of greenhouse gas emissions and the radiative forcing stabilizes at 4.5 W m⁻² in 2100 in the scenario. The RCP8.5 scenario, on the other hand, represents a world without any efficient mitigation activities applied and leads to almost twice as large forcing and warming on global scale by 2100. In Finland, the projected increases in mean annual temperature and precipitation are under the RCP8.5 scenario up to 6 °C and 18%, respectively, when the atmospheric CO₂ concentration approaches 1000 ppm by 2100 (Ruosteenoja et al., 2016). The increases in temperature and precipitation are both predicted to be much higher in winter months than in summer.

All the used bias-adjusted RCM simulations were constructed in the Institut Pierre Simon Laplace (IPSL) using a cumulative distribution function (CDF) method (Vrac et al., 2016). They were downscaled onto the EUR-11 CORDEX domain having a horizontal resolution of $\sim 0.11^\circ \times 0.11^\circ$ by using the Water and Global Change Forcing Data ERA Interim (WFDEI) meteorological forcing data set (Weedon et al., 2014) over a calibration period 1979–2014. The variables used in this study were daily mean 2-m air temperature and daily precipitation sum. Before soil temperature calculations, we performed for the GCM data a combined statistical downscaling and bias correction onto a regular $0.1^\circ \times 0.2^\circ$ grid covering Finland by applying a quantile mapping technique using smoothing (Räisänen and Räty, 2013; Räty et al., 2014). As our observational calibration data in the downscaling, we used gridded Finnish climate data set with 10 km horizontal resolution for the period 1981–2010 (Aalto et al., 2016). Before the calculations, also the RCM data were linearly interpolated onto the same $0.1^\circ \times 0.2^\circ$ grid.

3 Results

3.1 Wintertime bearing capacity during the baseline period 1981–2010

Fig. 2 shows the modelled annual average number of days with good wintertime bearing capacity during 1981–2010 in three different forest types common in Finland, i.e. dense Norway spruce (*Picea abies*) forests on clay or silt soil, Scots pine (*Pinus sylvestris*) forests on sandy soil and Scots pine forests on peatlands. The number of days with good wintertime bearing capacity on forest truck roads is shown as well. Upland forests on sandy soil generally have most and forests on drained peatlands least days with good bearing capacity as the soil frost penetrates fastest in sand and slowest in peat. The winter period with good bearing capacity lasts in northern Finland on average approximately 5–7 months, depending on forest and soil type. In the central parts of the country, the wintertime bearing season lasts about 3–4 months on drained peatlands and roughly about 5 months on other soil types. In the coastal areas of southern and southwestern Finland, the length of bearing season varies typically between 2 and 4 months per winter depending on the soil type. On forest truck roads, the bearing season is modelled to last about 3–4 months per winter in southern Finland and about half a year in northernmost Finland.

The used models generally reproduce the spatial pattern of wintertime bearing season length during the baseline period as expected as the model data has been bias-corrected. There are some small differences in the pattern between the



GCM and RCM ensembles, for example, the used RCMs tend to overestimate the length of bearing season along the coast of Bothnian Bay.

3.2 Wintertime bearing capacity during the future periods 2021–2050 and 2070–2099

The projected change in the average wintertime bearing season length for the above-mentioned forest types and for forest truck roads is displayed in Fig. 3 on the basis of the GCM ensemble and in Fig. 4 based on the RCM ensemble. The wintertime bearing season is projected to shorten roughly by about one month for the near-future period 2021–2050. The change is somewhat smaller under the RCP4.5 than RCP8.5 scenario. The GCM and RCM ensembles indicate rather similar changes. The projected change is moreover very similar among the different soil types. In northern Finland, the projected shortening of bearing season is most pronounced on drained peatlands, opposite to in southern Finland.

For the far-future period 2070–2099 the projected shortening of the wintertime bearing season is clearly more pronounced. In addition, the difference in the magnitude of change between the two forcing scenarios becomes larger. If the high-emission RCP8.5 scenario will be realized, the bearing season may shorten by more than 3 months over large parts of the country. On drained peatlands, the change remains smaller in southern Finland as the bearing season lasts there less than 3 months per winter already during the baseline period. On the other hand, in upland forests on sandy and clay or silt soil types the projected shortening of bearing season is largest in southern and western Finland. In these areas, the bearing season is projected to shorten by about 2 months also under the RCP4.5 scenarios.

The projected change in the wintertime bearing season length on forest truck roads accompanies the projected change on different forest types, especially on sandy and clay or silt soil types. By mid-century, the wintertime bearing season on forest truck roads may shorten by more than one month in western Finland. In the end of the 21st century, the bearing season on forest truck roads may last even on average only about one month per winter in the southwestern parts of the country of the RCP8.5 scenario will be realized.

3.3 Interannual variability in the wintertime bearing season length

Interannual variability in the wintertime bearing season length is illustrated in Fig. 5. Here we show the results only derived from the GCM ensemble and only for pine forests on drained peatlands as they are the most difficult sites for forest harvesting. During the baseline period, the bearing season length exceeds one month on more than 80% of the winters except in the coastal areas in southern and southwestern Finland (Fig. 5d). In Lapland, the bearing season lasts even on the mildest winters 2–3 months but at the southwestern coast, the mildest winters do not express good bearing capacity on any day (Fig. 5c). During the near-future period 2021–2050, the share of winters with less than one month of good bearing capacity is projected to somewhat increase, particularly in southern and western Finland (Figs 5h and 5l). However, over most of Finland a large majority of winters still have a sufficient amount of days with good bearing capacity, although the conditions during the mildest winters are projected to become more difficult. For the far-future period 2070–2099, the situation is projected to change more considerably, particularly if the RCP8.5 scenario will be realized (Figs 5q–5t). Based on the multi-GCM mean, only a few



winters express longer than one month bearing season in southern and western Finland (Fig. 5t). Even in eastern Finland and southwestern Lapland the bearing season length is projected to exceed one month approximately only on every other winter. During the mildest winters, soil frost may penetrate to 20 cm or snow depth exceed 40 cm only on localized areas in northern Finland.

5 3.4 Intermodel variability in the projected wintertime bearing season length

In Fig. 6 we illustrate the range of possible outcomes between different climate model projections for wintertime bearing season length in pine forests on drained peatlands. We have plotted the highest and lowest annual mean number of days with good wintertime bearing capacity among the used climate models on each grid cell over the two 30-year future periods under the two forcing scenarios, separately for the 6 GCMs and for the 11 RCMs. It is visible that already during the near-future period 2021–2050, the projected average wintertime bearing season length diverges by more than one month in both model ensembles. During the far-future period 2070–2099, the range in the average bearing season length among the model projections is typically already more than two months. The models with strongest warming even indicate that the average bearing season length in the end of the 21st century might be 0 days at the southwestern coast of Finland meaning that even during the coldest winters soil frost would not penetrate to 20 cm. The coldest model projections, on the other hand, indicate that the wintertime bearing season length would shorten only by about one month by the end of the 21st century.

4 Discussion and conclusions

4.1 Evaluation of methodology

The bearing capacity of forest soils was evaluated on the basis of soil temperature model that had been previously applied successfully in Finnish and Swedish conditions (Rankinen et al., 2004; Jungqvist et al., 2014). In this study, the model parameters were optimized separately for three different soil types based on soil temperature observations. Typically the model explained 90–99% of the observed soil temperature variability. However, on most of the locations the model tended to overestimate the frost formation and soil temperature variations near the surface.

The effect of forest density on soil frost formation was taken into account in the modelling of snow depth. The snow model was first optimized for open areas similarly as the soil temperature model. The effect of forest density on the snow depth was then evaluated based on literature. In general, snow depth decreases with increasing forest density. In our calculations this led to somewhat enhanced soil frost formation in denser forests. In reality, vegetation in forests also acts as an insulator. Thus, open areas often have deeper soil frost than forests despite of having also deeper snowpack, but the results from different sites are contradictory (Soveri and Varjo, 1977). According to Yli-Vakkuri (1960) soil frost penetrates particularly deep in dense spruce forests due to their large canopy cover leading to shallow snow depths.



The climate change impact on wintertime bearing capacity of forest soils was taken into account by using climate model simulations. We used both statistically downscaled and bias-corrected GCM data as well as dynamically downscaled and bias-adjusted RCM data. In our calculations, the climate data was downscaled onto $0.1^\circ \times 0.2^\circ$ (approximately $10 \text{ km} \times 10 \text{ km}$) grid. By combining the soil and vegetation information with the soil frost calculations, the expected changes in timber harvesting conditions can be evaluated in a relatively small scale. However, in reality there is considerable variability in the soil frost conditions also within relatively similar vegetation types. For example, the level of groundwater has a substantial impact on the soil frost depth (Soveri and Varjo, 1977). These kind of small-scale variations could not be taken into account in our idealized approach although the results are presented in a relatively high-resolution grid. Despite of many uncertainties in soil frost modelling, our results were in general reasonable. For instance, Eeronheimo (1991) stated that in drained peatlands the requirement of 20 cm of frost or 40 cm of snow cover on unfrozen ground results in an operating period of 60 days in southern Finland and 160 days in northern Finland. This accords almost perfectly well with our results for bearing season length during the baseline period in drained (pine dominated) peatlands (see Fig. 2g).

Considering the future projections, the two used climate model ensembles we used yielded rather similar results (Figs. 3 and 4) including increasing scatter among the model projections towards the end of the century (Fig. 6). The RCM ensemble using WFDEI forcing data set (Weedon et al., 2014) in bias correction had some differences in spatial small-scale features of bearing season length pattern compared to the GCM ensemble that used in bias correction the gridded Finnish climate data set (Aalto et al., 2016). Most notably, the RCMs produced longer soil frost periods along the coast of Bothnian Bay. Nevertheless, both model ensembles reproduced after the bias correction satisfactorily the general large-scale pattern of bearing season length when compared to the results calculated from observation-based gridded climate data (Fig. 2).

4.2 Evaluations of main results and their implications to forestry

In accordance with previous studies (Venäläinen et al., 2001a, 2001b; Kellomäki et al., 2010), our results suggest that climate warming will lead to shorter soil frost periods reducing wintertime ground-bearing capacity. The projected decrease in the wintertime bearing season length was similar in the studied two climate model ensembles. Most likely the bearing season length in winter will decrease by about one month until mid-21st century and by about 1.5–3 months until 2100. Nevertheless, there is considerable variation in the rate of the projected change among the individual climate model simulations.

In relative terms, the decrease in the wintertime bearing season length is most prominent in southern and western Finland. That is because in Lapland the season is typically three months longer than at the southern coast and thus even the most extreme projections do not lead to a complete loss of the ground frost there. Similarly, abilities for wintertime logging on drained peatlands are expected to worsen more than on upland soil types. Based on our results it is evident that in the latter half of the century on drained peatlands logging cannot be expected to be conducted during frozen soil conditions in most parts of Finland. On the other hand, shortening of the soil frost season leads to an earlier transition to summer conditions. This leads



to a reduced soil moisture content in spring and also in summer the soil moisture content is projected most likely to decrease (Ruosteenoja et al., 2017). Consequently, possibilities for summertime logging may improve.

Our results considering the climate change impact on the conditions of forest harvesting and logistics provide urgently needed support for the planning of wood harvesting and transportation in different timespans and regions. During the last 5 couple of decades, there has also been a trend towards heavier machinery in forest harvesting (Ala-Ilomäki et al., 2011) and the allowed maximum weight of timber trucks has increased (e.g., Malinen et al., 2014). The forest truck roads in Finland have been mainly constructed between 1960 and 1990 and many of them need a major renovation before timber haulage can take place (Kaakkurivaara et al., 2005). Hence, maintaining sufficient bearing capacity on forest truck road network is also important. Fortunately, there are several possibilities to improve mobility of forest machinery on poorly bearing conditions. 10 For example, the carrying surface can be extending by using auxiliary wheels, width of individual wheels can be widened, tyre pressure can be reduced or wider tracks can be used (Airavaara et al., 2008). One possibility is also to use two-stage wood harvesting. In this method, the cutting is conducted when the soil is still unfrozen but wood stacks are extracted later in winter when the soil is frozen (Heikkilä, 2007). Logging residues can be placed on the forwarding trails to improve the soil bearing capacity as is done in Northern Scotland on peatland harvesting (Röser et al. 2011). This, however, reduces the volume of 15 harvestable logging residues for energy use. Anyway, as there is a pressure to increase wood harvesting in drained peatlands in the future with simultaneous decrease in the ground-bearing capacity, there is a clear need to develop new cost-effective solutions for peatland harvesting, taking into account this anticipated decrease in ground-bearing capacity.

4.3 Conclusions

The results of this study indicate clearly that the soil frost period in Finland will become shorter as climate becomes warmer. 20 Hence, it is evident that a larger share of logging need to be carried out under unfrozen soil conditions. Particularly this holds for drained peatlands as the soil frost period is there shortest due to the insulating effect of peat. In southern and western Finland, drained peatlands might remain virtually frost-free on most of winters during the latter half of the current century. Already by 2050, the winters with only short frost periods will become more common. The projected decrease in the bearing capacity, particularly in drained peatlands, with simultaneously increasing demand for the wood utilization from peatlands 25 induces a clear need for the development of new sustainable and efficient logging practices. To foster the use of our results, the data showing the average bearing season length in different combinations of soil and forest types during different study periods will be made publicly available.

The results presented here will also serve as a basis for several future analysis. The effects of changing climate on timber procurement in different regions of Finland should be analysed in more detail. In addition, it should be analysed what 30 kind of supply technology development needs exist concerning logging machinery, transportation fleet and information systems managing and monitoring the raw material flows in the future. These soil frost calculations can be also applied in studying climate change impacts on wind damage risks to forests as soil frost makes trees more resistant for uprooting by



anchoring them effectively to the ground (Peltola et al., 1999; Saad et al., 2017). With regard to harvesting logistics, it would be interesting to study also whether clear cutting facilitates the transformation of some peatland stands marked for cutting in winter into stands marked for cutting in summer (Ala-Ilomäki et al. 2011, Sirén et al. 2013, Laitila et al. 2016). This is because, compared to thinning, clear cutting allows greater freedom in the location of forwarding routes on site, as well as in organising route schedules (Uusitalo et al. 2015b).

5

5. Data availability

The climate model data used in this study can be downloaded from the CMIP5 and CORDEX archives, e.g. at <https://esgf-node.ipsl.upmc.fr/projects/esgf-ipsl/>. The observational gridded Finnish climate data from 1961 onwards can be downloaded from the Paituli spatial data download service at <http://avaa.tdata.fi/web/paituli/metadata>. The soil temperature observations 10 from the stations listed in Table 1 are available on request from the corresponding author. The spatial data describing the multi-GCM mean wintertime bearing season length on different combinations of soil and forest types over the studied periods will be made available at the Paituli spatial data download service after the publication of this paper.

10

Acknowledgments

15 This research has been supported by the Strategic Research Council at the Academy of Finland through the FORBIO (Sustainable, climate-neutral, and resource-efficient forest-based bioeconomy) research project (grant numbers 293380 and 314224). We acknowledge the World Climate Research Programme's Working Group on Regional Climate and Working Group on Coupled Modelling, former coordinating body of the CORDEX project and latter being responsible for CMIP. We are moreover grateful to all the modelling groups (listed in Tables S3 and S4 in the supplementary material of this paper) for 20 producing and making their model outputs available. The model data used in this work were obtained from the Earth System Grid Federation portal. For CMIP the US Department of Energy's Program for Climate Model Diagnosis and Intercomparison provides coordinating support and led development of software infrastructure in partnership with the Global Organization for Earth System Science Portals. Kimmo Ruosteenoja is acknowledged for downloading and preprocessing the GCM data. Olle Räty and Jouni Räisänen from Department of Physics, University of Helsinki, are acknowledged for developing the bias 25 correction software applied on the GCM data.

25

References

Aalto, J., Pirinen, P. and Jylhä, K.: New gridded daily climatology of Finland: Permutation-based uncertainty estimates and temporal trends in climate. *Journal of Geophysical Research: Atmospheres*, 121, 3807–3823, doi:10.1002/2015JD024651, 2016.

30



Airavaara, H., Ala-Ilomäki, J., Högnäs, T. and Sirén, M.: Nykykalustolla turvemaiden puunkorjuuseen [Equipping conventional wheeled forwarders for peatland operations], Working Papers of the Finnish Forest Research Institute 80. 46 pp., 2008.

5 Ala-Ilomäki, J., Högnäs, T., Lamminen, S. and Siren, M.: Equipping a conventional wheeled forwarder for peatland operations. International Journal of Forest Engineering, 22(1), 7–13, 2011.

Anderson, E. A.: National Weather Service Forecast System-Snow Accumulation and Ablation model, NOAA Technical Memorandum NWS HYDRO-17, U.S. Dept. of Commerce, Silver Spring, MD, 217 pp., 1973.

10

Asikainen, A., Mutanen, A., Kangas, A., Vehmasto, E., Verkasalo, E., Ylitalo, E., Hynynen, J., Viitanen, J., Backman, J., Laitila, J., Korhonen, K.T., Finér, L., Neuvonen, M., Kurtila, M., Peltoniemi, M., Salminen, O., Peltonen-Sainio, P., Peltola, R., Korpinen, R., Kurppa, S., Räty, T., Saksa, T., Sievänen, T., Packalen, T., Saarinen, V.-M., Kankaanhauta, V. and Kolttola, L.: Vihreä biotalous: 100-vuotiaan Suomen hyvinvoinnin ja kilpailukyvyn perusta, edited by: Jaakkonen, A.-K. and Ylitalo, E., Luonnonvara- ja biotalouden tutkimus 59/2016, 25 pp., 2016.

15

Carroll, M. J., Dennis, P., Pearce-Higgins, J. W. and Thomas, C. D.: Maintaining northern peatland ecosystems in a changing climate: effects of soil moisture, drainage and drain blocking in craneflies, Global Change Biology, 17, 2991–3001, doi:10.1111/j.1365-2486.2011.02416.x, 2011.

20

Collins, M., Knutti, R., Arblaster, J., Dufresne, J.-L., Fichefet, T., Friedlingstein, P., Gao, X., Gutowski, W. J., Johns, T., Krinner, G., Shongwe, M., Tebaldi, C., Weaver, A. J. and Wehner, M.: Long-term climate change: projections, commitments and irreversibility, in: The Physical Science Basis, Contribution of Working Group I to the Fifth Assessment Report of the Intergovernmental Panel on Climate Change, edited by: Stocker, T. F., Qin, D., Plattner, G.-K., Tignor, M., Allen, S. K., Boschung, J., Nauels, A., Xia, Y., Bex, V. and Midgley, P. M., Cambridge University Press, Cambridge and New York, 1029–1136, 2013.

25

Eeronheimo, O.: Suometsien puunkorjuu – Forest harvesting on peatlands, Folia Forestalia 779, The Finnish Forest Research Institute, 29 pp., available at: <https://core.ac.uk/download/pdf/52273561.pdf>, last access: 12 December 2017, 1991.

30

Finnish Forest Research Institute: Finnish Statistical Yearbook of Forestry, Tammerprint, Tampere, 428 pp, 2014.

Flato, G., Marotzke, J., Abiodun, B., Braconnot, P., Chou, S. C., Collins, W., Cox, P., Driouech, F., Emori, S., Eyring, V., Forest, C., Gleckler, P., Guilyardi, E., Jakob, C., Kattsov, V., Reason, C. and Rummukainen, M.: Evaluation of Climate Models, in: Climate Change 2013: The Physical Science Basis. Contribution of Working Group I to the Fifth Assessment Report of the Intergovernmental Panel on Climate Change, edited by: Stocker, T. F., Qin, D., Plattner, G.-K., Tignor, M., Allen, S. K., Boschung, J., Nauels A., Xia, Y., Bex, V. and Midgley, P. M., Cambridge University Press, Cambridge and New York, 741–866, 2013

40

Gurevich, M. I.: Dependence of the snow melting rate on air temperature, Meteorology and Hydrology (Meteorologiya i gidrologiya), No. 3, 44–48, 1950.

Hankimo, J.: Sateen olomuodon prediktoreista, Finnish Meteorological Institute, tutkimusseloste 57, 1976.

45

Hedstrom, N. R. and Pomeroy, J. W.: Measurements and modelling of snow interception in the boreal forest, Hydrological Processes, 12, 1611–1625, doi:10.1002/(SICI)1099-1085(199808/09)12:10/11<1611::AID-HYP684>3.0.CO;2-4, 1998.

Heikinheimo, M. and Fougstedt, B.: Statistics of soil temperature in Finland 1971–1990, Meteorological Publications, Finnish Meteorological Institute, Painatuskeskus Oy, Helsinki, 75 pp., 1992.

50



Heikkilä, J.: Turvemaiden puun kasvatus ja korjuu – nykytila ja kehittämistarpeet [Silviculture and harvesting of peatland forests - the current state and future development needs], Working Papers of the Finnish Forest Research Institute 43, 29 pp., 2007.

5 Hiitiö, M.: Lumen sulannasta ja sen aiheuttaman valunnan arvioinnista, M.Sc. thesis, Department of Civil Engineering, Helsinki University of Technology, Finland, 96 pp., 1982.

Houle, D., Bouffard, A., Duchesne, L., Logan, T. and Harvey, R.: Projections of future soil temperature and water content for three southern Quebec forested sites, *J. Climate*, 25, 7690–7701, doi:10.1175/JCLI-D-11-00440.1, 2012.

10

Jacob, D., Petersen, J., Eggert, B., Alias, A., Christensen, O. B., Bouwer, L. M., Braun, A., Colette, A., Déqué M., Georgievski, G., Georgopoulou, E., Gobiet, A., Menut, L., Nikulin, G., Haensler, A., Hempelmann, N., Jones, C., Keuler, K., Kovats, S., Kröner, N., Kotlarski, S., Kriegsmann, A., Martin, E., van Meijgaard, E., Moseley, C., Pfeifer, S., Preuschmann, S., Radermacher, C., Radtke, K., Rechid, D., Rounsevell, M., Samuelsson, P., Somot, S., Soussana, J.-F., Teichmann, C., 15 Valentini, R., Vautard, R., Weber, B. and Yiou, P.: EURO-CORDEX: new high-resolution climate change projections for European impact research, *Regional Environmental Change*, 14, 563–578, doi:10.1007/s10113-013-0499-2, 2014.

Jansson, P.-E.: CoupModel: model use, calibration, and validation. *Trans. ASABE*, 55, 1335–1344, 2012.

20

Jungqvist, G., Oni, S. K., Teutschbein, C. and Futter, M. N.: Effect of climate change on soil temperature in Swedish boreal forests, *PLoS ONE* 9(4): e93957, doi:10.1371/journal.pone.0093957, 2014.

Kaakkurivaara T., Vuorimies N., Kolisoja P. and Uusitalo, J.: Applicability of portable tools in assessing the bearing capacity of forest roads, *Silva Fennica*, 49, 1239, doi:10.14214/sf.1239, 2015.

25

Kellomäki, S., Maajärvi, M., Strandman, H., Kilpeläinen, A. and Peltola, H.: Model computations on the climate change effects on snow cover, soil moisture and soil frost in the boreal conditions over Finland, *Silva Fennica*, 44, 213–233, doi:10.14214/sf.455, 2010.

30

Komulainen, V.-M., Tuittila, E.-S., Vasander, H. and Laine, J.: Restoration of drained peatlands in southern Finland: initial effects on vegetation change and CO₂ balance, *Journal of Applied Ecology*, 36, 634–648, doi:10.1046/j.1365-2664.1999.00430.x, 1999.

35

Knutti, R. and Sedláček, J.: Robustness and uncertainties in the new CMIP5 climate model projections, *Nature Climate Change*, 3, 369–373, doi:10.1038/nclimate1716, 2013.

Laitila, J., Väätäinen, K. and Asikainen, A.: Comparison of two harvesting methods for complete tree removal on tree stands on drained peatlands, *Suo*, 64, 77–95, 2013.

40

Lundberg, A. and Koivusalo, H.: Estimating winter evaporation in boreal forests with operational snow course data. *Hydrological Processes*, 17, 1479–1493, doi:10.1002/hyp.1179, 2003.

Malinen, J., Nousiainen, V., Palojärvi, K. and Palander, T.: Prospects and challenges of timber trucking in a changing operational environment in Finland, *Croatian Journal of Forest Engineering*, 35, 91–100, 2014.

45

Manner, J., Gelin, O., Mörk, A. and Englund, M.: Forwarder crane's boom tip control system and beginner-level operators. *Silva Fennica*, 51, 1717, doi:10.14214/sf.1717, 2017.



Ministry of Employment and the Economy, Ministry of Agriculture and Forestry, and Ministry of the Environment: Sustainable growth from bioeconomy – The Finnish bioeconomy strategy, Edita Prime Ltd, 17 pp., available at: http://biotalous.fi/wp-content/uploads/2014/08/The_Finnish_Bioeconomy_Strategy_110620141.pdf, last access: 12 December 2017, 2014.

5 Natural Resources Institute Finland: Forest industries' wood consumption 2016, available at: http://stat.luke.fi/en/forest-industries-wood-consumption-2016_en, last access: 12 December 2017, 2017a.

Natural Resources Institute Finland: Finnish roundwood harvests to a record level in 2016, available at: <https://www.luke.fi/en/news/finnish-roundwood-harvests-record-level-2016/>, last access: 12 December 2017, 2017b.

10 10 Nugent, C., Kanali, C., Owende, P. M. O., Nieuwenhuis, M. and Ward, S.: Characteristic site disturbance due to harvesting and extraction machinery traffic on sensitive forest sites with peat soils, *Forest Ecology and Management*, 180, 85–98, doi:10.1016/S0378-1127(02)00628-X, 2003.

15 15 Nurminen, T., Korpunen, H. and Uusitalo, J.: Time consumption analysis of the mechanized cut-to-length harvesting system, *Silva Fennica*, 40, 335–363, doi:10.14214/sf.346, 2006.

Nurminen, T. and Heinonen, J.: Characteristics and time consumption of timber trucking in Finland, *Silva Fennica*, 41, 471–487, doi:10.14214/sf.284, 2007.

20 20 Oni, S. K., Mieres, F., Futter, M. N. and Laudon, H.: Soil temperature responses to climate change along a gradient of upland-riparian transect in boreal forest, *Climatic Change*, 143, 27–41, doi:10.1007/s10584-017-1977-1, 2017.

25 25 Park, S. K., Sungmin, O. and Cassardo, C.: Soil temperature response in Korea to a changing climate using a land surface model, *Asia-Pac. J. Atmos. Sci.*, 53, 457–470, doi:10.1007/s13143-017-0048-x, 2017.

Peltola, H., Kellomäki, S. and Väistänen, H.: Model computations of the impact of climatic change on the windthrow risk of trees, *Climatic Change* 41, 17–36, doi:10.1023/A:1005399822319, 1999.

30 30 Pitkänen, A., Turunen, J., Tahvanainen, T. and Simola, H.: Carbon storage change in a partially forestry-drained boreal mire determined through peat column inventories, *Boreal Environmental Research*, 18, 223–234, 2013.

35 35 Pohjankukka, J., Riihimäki, H., Nevalainen, P., Pahikkala, T., Ala-Ilomäki, J., Hyvönen, E., Varjo, J. and Heikkonen, J.: Predictability of boreal forest soil bearing capacity by machine learning, *Journal of Terramechanics*, 68, 1–8, doi:10.1016/j.jterra.2016.09.001, 2016.

Räisänen, J. and Räty, O.: Projections of daily mean temperature variability in the future: cross-validation tests with ENSEMBLES regional climate models, *Climate Dynamics*, 41, 1553–1568, doi:10.1007/s00382-012-1515-9, 2013.

40 40 Räisänen, J. and Ylhäisi, J. S.: CO₂-induced climate change in northern Europe: CMIP2 versus CMIP3 versus CMIP5, *Climate Dynamics*, 45, 1877–1897, doi:10.1007/s00382-014-2440-x, 2015.

45 45 Rankinen, K., Karvonen, T. and Butterfield, D.: A simple model for predicting soil temperature in snow-covered and seasonally frozen soil: model description and testing, *Hydrology and Earth System Sciences*, 8, 706–716, doi:10.5194/hess-8-706-2004, 2004.

50 50 Rasmus, S., Gustafsson, D., Koivusalo, H., Laurén, A., Grelle, A., Kauppinen, O.-K., Lagnvall, O., Lindroth, A., Rasmus, K., Svensson, M. and Weslien, P.: Estimation of winter leaf area index and sky view fraction for snow modelling in boreal coniferous forests: consequences on snow mass and energy balance. *Hydrological Processes*, 27, 2876–2891, doi:10.1002/hyp.9432, 2013.



Räty, O., Räisänen, J. and Ylhäisi J. S.: Evaluation of delta change and bias correction methods for future daily precipitation: intermodel cross-validation using ENSEMBLES simulations, *Climate Dynamics*, 42, 2287–2303, doi:10.1007/s00382-014-2130-8, 2014.

5

Röser, D., Sikanen, L., Asikainen, A., Parikka, H. and Väätäinen, K.: Productivity and cost of mechanized energy wood harvesting in Northern Scotland, *Biomass and Bioenergy*, 35, 4570–4580, doi:10.1016/j.biombioe.2011.06.028, 2011.

Ruosteenoja, K., Jylhä, K. and Kämäräinen, M.: Climate projections for Finland under the RCP forcing scenarios, *Geophysica*, 10 51, 17–50, 2016.

Ruosteenoja, K., Markkanen, T., Venäläinen, A., Räisänen, P. and Peltola, H.: Seasonal soil moisture and drought occurrence in Europe in CMIP5 projections for the 21st century, *Climate Dynamics*, doi:10.1007/s00382-017-3671-4, in press, 2017.

15 Saad, C., Boulanger, Y., Beaudet, M., Gachon, P., Ruel, J.-C. and Gauthier, S.: Potential impact of climate change on the risk of windthrow in eastern Canada's forests, *Clim. Change*, 143, 487–501, doi:10.1007/s10584-017-1995-z, 2017.

Simola, H., Pitkänen, A. and Turunen, J.: Carbon loss in drained forestry peatlands in Finland, estimated by resampling peatlands surveyed in the 1980s, *European Journal of Soil Science*, 63, 798–807, doi:10.1111/j.1365-2389.2012.01499.x, 20 2012.

Sinha, T. and Cherkauer, K. A.: Impacts of future climate change on soil frost in the Midwestern United States, *J. Geophys. Res.*, 115, D08105, doi:10.1029/2009JD012188, 2010.

25 Sirén, M., Ala-Ilomäki, J., Mäkinen, H., Lamminen, S. and Mikkola, T.: Harvesting damage caused by thinning of Norway spruce in unfrozen soil, *International Journal of Forest Engineering*, 24, 60–75, doi:10.1080/19132220.2013.792155, 2013.

Soveri, J. and Varjo, M.: Roudan muodostumisesta ja esiintymisestä Suomessa vuosina 1955–1975, *Publications of the Water Research Institute, National Board of Waters, Valtion Painatuskeskus*, Helsinki, 66 pp., 1977.

30

Stähli, M. and Gustafsson, D.: Long-term investigations of the snow cover in a subalpine semi-forested catchment, *Hydrological Processes*, 20, 411–428, doi:10.1002/hyp.6058, 2006.

35 Suvinen, A.: A GIS-based simulation model for terrain tractability, *Journal of Terramechanics*, 43, 427–449, doi:10.1016/j.terra.2005.05.002, 2006.

Svenson, G. and Fjeld, D.: The impact of road geometry and surface roughness on fuel consumption of logging trucks, *Scandinavian Journal of Forest Research*, 31, 526–536, doi:10.1080/02827581.2015.1092574, 2016.

40 Taylor, K. E., Stouffer, R. J. and Meehl, G. A.: An overview of CMIP5 and the experimental design, *Bulletin of the American Meteorological Society*, 93, 485–498, doi:10.1175/BAMS-D-11-00094.1, 2012.

45

Uusitalo, J. and Ala-Ilomäki, J.: The significance of above-ground biomass, moisture content and mechanical properties of peat layer on the bearing capacity of ditched pine bogs, *Silva Fennica*, 47, 993, doi:10.14214/sf.993, 2013.

50 Uusitalo J., Salomäki M. and Ala-Ilomäki J.: Variation of the factors affecting soil bearing capacity of ditched pine bogs in Southern Finland, *Scandinavian Journal of Forest Research*, 30, 429–439, doi:10.1080/02827581.2015.1012110, 2015a.



Uusitalo, J., Salomäki, M. and Ala-Ilomäki, J.: The effect of wider logging trails on rut formation in the harvesting of peatland forests, Croatian Journal of Forest Engineering, 36, 125–130, 2015b.

5 van Vuuren, D. P., Edmonds, J., Kainuma M., Riahi, K., Thomson, A., Hibbard, K., Hurtt, G. C., Kram, T., Krey, V., Lamarque, J.-F., Masui, T., Meinshausen, M., Nakicenovic, N., Smith, S. J. and Rose, S. K.: The representative concentration pathways: an overview, Climatic Change, 109, 5–31, doi:10.1007/s10584-011-0148-z, 2011.

10 Varhola, A., Coops, N. C., Weiler, M. and Dan Moore, R.: Forest canopy effects on snow accumulation and ablation: An integrative review of empirical results, Journal of Hydrology, 392, 219–233, doi:10.1016/j.jhydrol.2010.08.009, 2010.

Vehviläinen, B.: Snow cover models in operational watershed forecasting, Publications of the Water and Environment Research Institute, National Board of Waters and the Environment, Valtion Painatuskeskus, Helsinki, 112 pp., 1992.

15 Venäläinen, A., Tuomenvirta, H., Heikinheimo, M., Kellomäki, S., Peltola, H., Strandman, H. and Väisänen, H.: Impact of climate change on soil frost under snow cover in a forested landscape, Climate Research, 17, 63–72, doi:10.3354/cr017063, 2001a.

20 Venäläinen, A., Tuomenvirta, H., Lahtinen, R. and Heikinheimo, M.: The influence of climate warming on soil frost on snow-free surfaces in Finland, Climatic Change, 50, 111–128, doi:10.1023/A:1010663429684, 2001b.

Vrac, M., Noël, T. and Vautard, R.: Bias correction of precipitation through Singularity Stochastic Removal: Because occurrences matter, Journal of Geophysical Research: Atmospheres, 121, 5237–5258, doi:10.1002/2015JD024511, 2016.

25 Weedon, G. P., Balsamo, G., Bellouin, N., Gomes, S., Best, M. J. and Viterbo, P.: The WFDEI meteorological forcing data set: WATCH Forcing Data methodology applied to ERA-Interim reanalysis data, Water Resources Research, 50, 7505–7514, doi:10.1002/2014WR015638, 2014.

30 Wolfsmayr, U.J. and Rauch, P.: The primary forest fuel supply chain: A literature review, Biomass and Bioenerg, 60, 203–221, doi:10.1016/j.biombioe.2013.10.025, 2014.

Yang, D., Goodison, B. E., Metcalfe, J. R., Louie, P., Leavesley, G., Emerson, D., Hanson, C. L., Golubev, V. S., Elomaa, E., Gunther, T., Pangburn, T., Kang, E. and Milkovic, J.: Quantification of precipitation measurement discontinuity induced by wind shields on national gauges, Water Resources Research, 35, 491–508, doi:10.1029/1998WR900042, 1999.

35 Yin, X. W., and Arp, P. A.: Predicting forest soil temperatures from monthly air temperature and precipitation records, Can. J. For. Res., 23, 2521–2536, doi:10.1139/x93-313, 1993.

Yli-Vakkuri, P.: Metsiköiden routa- ja lumisuhteista, Acta Forestalia Fennica, 71, 7114, doi:10.14214/aff.7114, 1960.



Table 1. Soil temperature measurement data used in the optimization of soil frost model.

Station name	Latitude	Longitude	Soil type	Soil temperature measurement depths	Observation period
Lettosuo	60°38'31"N	23°57'35"E	peat	5, 15, 30 and 40 cm	2009–2014
Anjala	60°41'47"N	26°48'40"E	clay/silt	10, 20, 30, 50, 70, 100, 150 and 200 cm	2007–2014
Jyväskylä	62°23'51"N	25°40'15"E	silt	10, 20, 30, 70, 100, 150 and 200 cm	2007–2014
Ylistaro	62°56'17"N	22°29'20"E	silt/clay	20, 50, 100, 200 and 300 cm	2007–2014
Maaninka	63°8'36"N	27°18'47"E	fine sand/silt	10, 20, 30, 50, 70, 100, 150 and 200 cm	2007–2014
Apukka	66°34'46"N	26°0'40"E	till	10, 20, 30, 50, 70, 100, 150 and 200 cm	2007–2014
Sodankylä	67°21'60"N	26°37'44"E	sand/gravel	10, 20, 30, 50, 70, 100, 150 and 200 cm	2007–2014
Lompolojännikä	67°59'50"N	24°12'33"E	peat	5, 15 and 30 cm	2007–2009
Kaamanen	69°8'26"N	27°16'11"E	peat	5, 15 and 30 cm	2004–2012
Kevo	69°45'23"N	27°0'24"E	sand	10, 20, 50, 100 and 200 cm	2007–2014



Table 2. Parameter ranges for the model optimization simulations.

Parameter	Unit	Sampling range
Soil thermal conductivity, K_T	$\text{W m}^{-1} \text{K}^{-1}$	0...2
Specific heat capacity of soil, C_S	$\text{J m}^{-3} \text{K}^{-1}$	0.5...3.5 (10^6)
Specific heat capacity due to freezing and thawing, C_{ICE}	$\text{J m}^{-3} \text{K}^{-1}$	4...15 (10^6)
Empirical snow parameter, f_S	m^{-1}	0...10
Lower soil thermal conductivity, $K_{T,LOW}$	$\text{W m}^{-1} \text{K}^{-1}$	0...1
Lower soil specific heat capacity, $C_{S,LOW}$	$\text{J m}^{-3} \text{K}^{-1}$	0.5...3.5 (10^6)
Lower soil temperature depth, Z_l	m	3...15

Table 3. Optimized parameters of soil temperature model for different soil types. The values of parameters are as follows:
 $a=25.7877098$, $b=0.18029317$, $c=0.71240088$, $d=-0.5861593$, $e=2.718281828459$, $f=0.3327189$, $g=18.2314362$,
 $h=0.17401331$, $i=1.08849685$, $j=-1.0702823$, $k=0.57526181$, $l=19.2170153$, $m=0.18221864$, $n=0.20835289$, $o=1.897$,
 $p=124.758$, $q=24.39751$, $r=0.4635642$, $s=0.01077341$, Z =soil depth (cm).

Parameter	Clay/Silt	Sand	Peat
Soil thermal conductivity, K_T ($\text{W m}^{-1} \text{K}^{-1}$)	$K_T = c/(1 + ae^{-bZ})$, when $Z < 8 \text{ cm}$ $K_T = d + f \ln Z$, when $Z \geq 8 \text{ cm}$	$K_T = i/(1 + ge^{-hZ})$, when $Z < 11 \text{ cm}$ $K_T = j + k \ln Z$, when $Z \geq 11 \text{ cm}$	$K_T = n/(1 + le^{-mZ})$
Specific heat capacity of soil, C_S ($\text{J m}^{-3} \text{K}^{-1}$)	C_S $= \left(r + \frac{o - r}{(1 + (Z/q)^p)^s} \right) \cdot 10^6$	C_S $= \left(r + \frac{o - r}{(1 + (Z/q)^p)^s} \right) \cdot 10^6$	C_S $= \left(r + \frac{o - r}{(1 + (Z/q)^p)^s} \right) \cdot 10^6$
Specific heat capacity due to freezing and thawing, C_{ICE} ($\text{J m}^{-3} \text{K}^{-1}$)	C_{ICE} $= 11.0 \cdot 10^6 \text{ J m}^{-3} \text{K}^{-1}$	C_{ICE} $= 7.0 \cdot 10^6 \text{ J m}^{-3} \text{K}^{-1}$	C_{ICE} $= 11.0 \cdot 10^6 \text{ J m}^{-3} \text{K}^{-1}$
Empirical snow parameter, f_S (m^{-1})	$f_S = 9.0 \text{ m}^{-1}$	$f_S = 9.0 \text{ m}^{-1}$	$f_S = 9.0 \text{ m}^{-1}$
Lower soil thermal conductivity, $K_{T,LOW}$ ($\text{W m}^{-1} \text{K}^{-1}$)	$K_{T,LOW}$ $= 0.8 \text{ W m}^{-1} \text{K}^{-1}$	$K_{T,LOW}$ $= 0.8 \text{ W m}^{-1} \text{K}^{-1}$	$K_{T,LOW}$ $= 0.8 \text{ W m}^{-1} \text{K}^{-1}$
Lower soil specific heat capacity, $C_{S,LOW}$ ($\text{J m}^{-3} \text{K}^{-1}$)	$C_{S,LOW}$ $= 1.8 \cdot 10^6 \text{ J m}^{-3} \text{K}^{-1}$	$C_{S,LOW}$ $= 1.8 \cdot 10^6 \text{ J m}^{-3} \text{K}^{-1}$	$C_{S,LOW}$ $= 1.8 \cdot 10^6 \text{ J m}^{-3} \text{K}^{-1}$
Lower soil temperature depth, Z_l (m)	$Z_l = 6.8 \text{ m}$	$Z_l = 6.8 \text{ m}$	$Z_l = 6.8 \text{ m}$



Table 4. Parameter ranges for snow model optimization and the optimized parameter values.

Parameter	Unit	Sampling range	Optimized value ¹
a	1	0.0...0.3	0.160975225
b	kg m ⁻³ °C ⁻¹	0...20	7.41216035
c	kg m ⁻³	100...250	218.46983092
cps	1	1.0...1.5	1.3065380539
tm	°C	-1.0...2.0	-0.4674846189
pm	°C ⁻¹ d ⁻¹	0.0...1.0	0.4355929409
ev	mm d ⁻¹	0.0...0.2	0.0787463821
kmax	mm °C ⁻¹ d ⁻¹	2.5...15.0	0.26291311* $e^{0.03958291*\lambda}$
kmin	mm °C ⁻¹ d ⁻¹	0.1...2.5	1044.72422* $e^{-0.1025652*\lambda}$
$\rho_{s,new,min}$	kg m ⁻³	30...100	60.42091336
$\rho_{s,max}$	kg m ⁻³	200...400	291.42990453
$\rho_{s,inc,rain}$	kg m ⁻³ mm ⁻¹ d ⁻¹	0...10	5.40364768
$\rho_{s,inc,age}$	kg m ⁻³ d ⁻¹	0...20	2.67193647
$\rho_{s,inc,thaw}$	kg m ⁻³ °C ⁻¹ d ⁻¹	0...20	6.22849401

¹ $e=2.718281828459$, λ =latitude in degrees north

Table 5. Interception coefficients, kmax coefficients and kmin coefficients used in this study for different forest types.

Forest density class	Interception coefficient	Kmax coefficient	Kmin coefficient
Open area	1.00	1.00	1.00
Deciduous forest / sparse mixed forest	0.92	0.65	0.875
Pine forest	0.86	0.60	0.85
Dense spruce forest	0.70	0.50	0.80

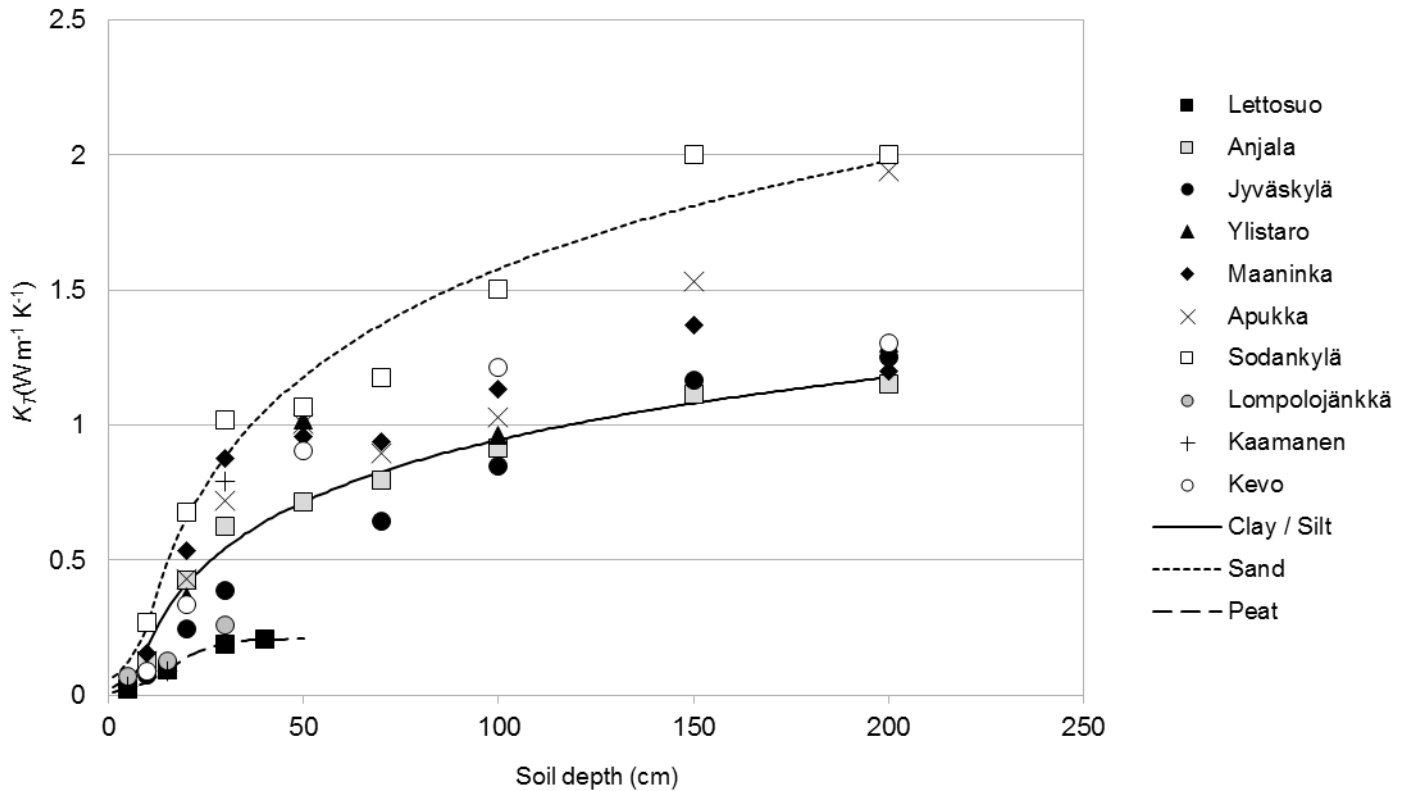


Figure 1. Optimized K_T values at each soil temperature measurement site and depth. Logistic regression curves fitted to the data from Anjala, Sodankylä and Lettosuo stations representing clay/silt, sand and peat soil types, respectively, are shown as well.

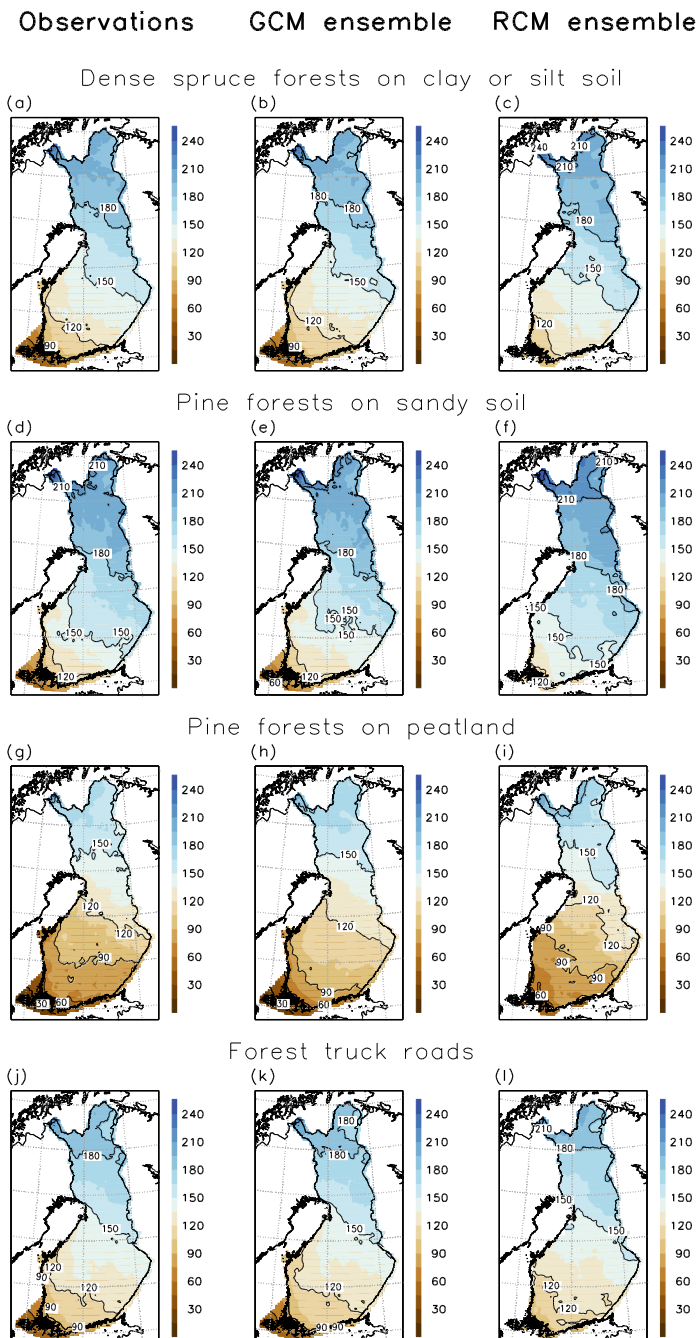


Figure 2. Annual average modelled number of days with good bearing capacity over the period 1981–2010 in three different forest and soil types and in forest truck roads based on observed weather data (left panel), bias-corrected GCM ensemble (middle panel) and bias-adjusted RCM ensemble (right panel).

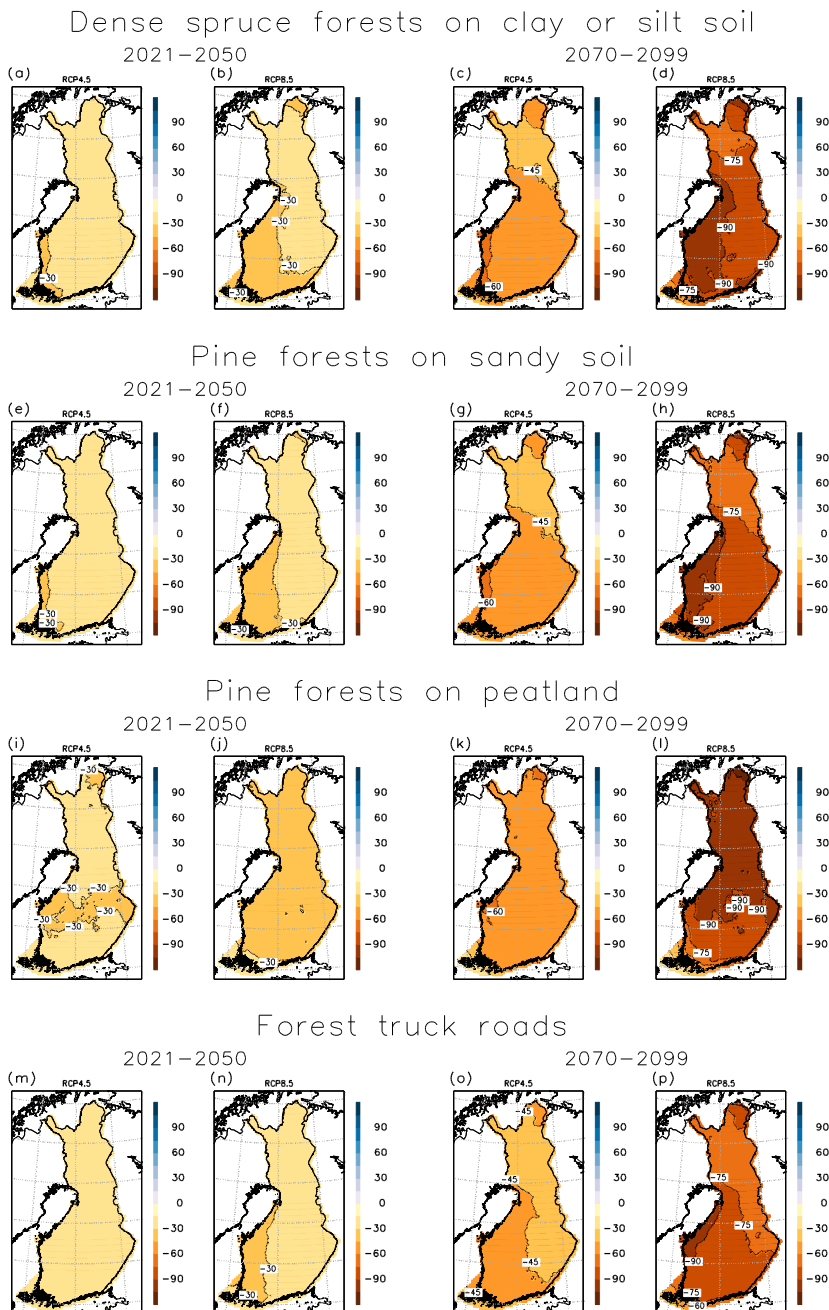


Figure 3. Projected multi-GCM mean change in the annual number of days with good bearing capacity in three different forest and soil types and in forest truck roads from 1981–2010 to 2021–2050 and to 2070–2099 under the RCP4.5 and RCP8.5 scenarios.

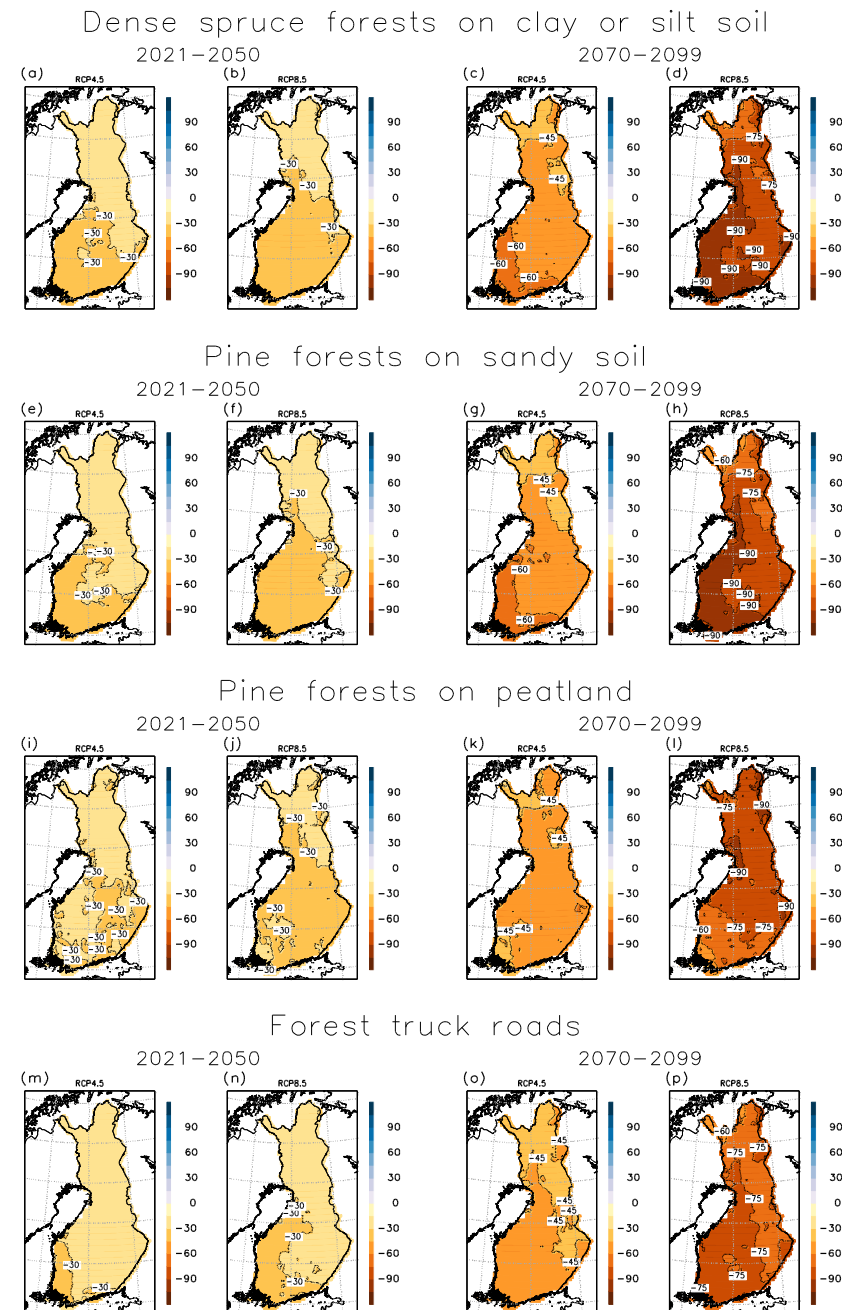


Figure 4. As in Fig. 3 but for multi-RCM mean change.

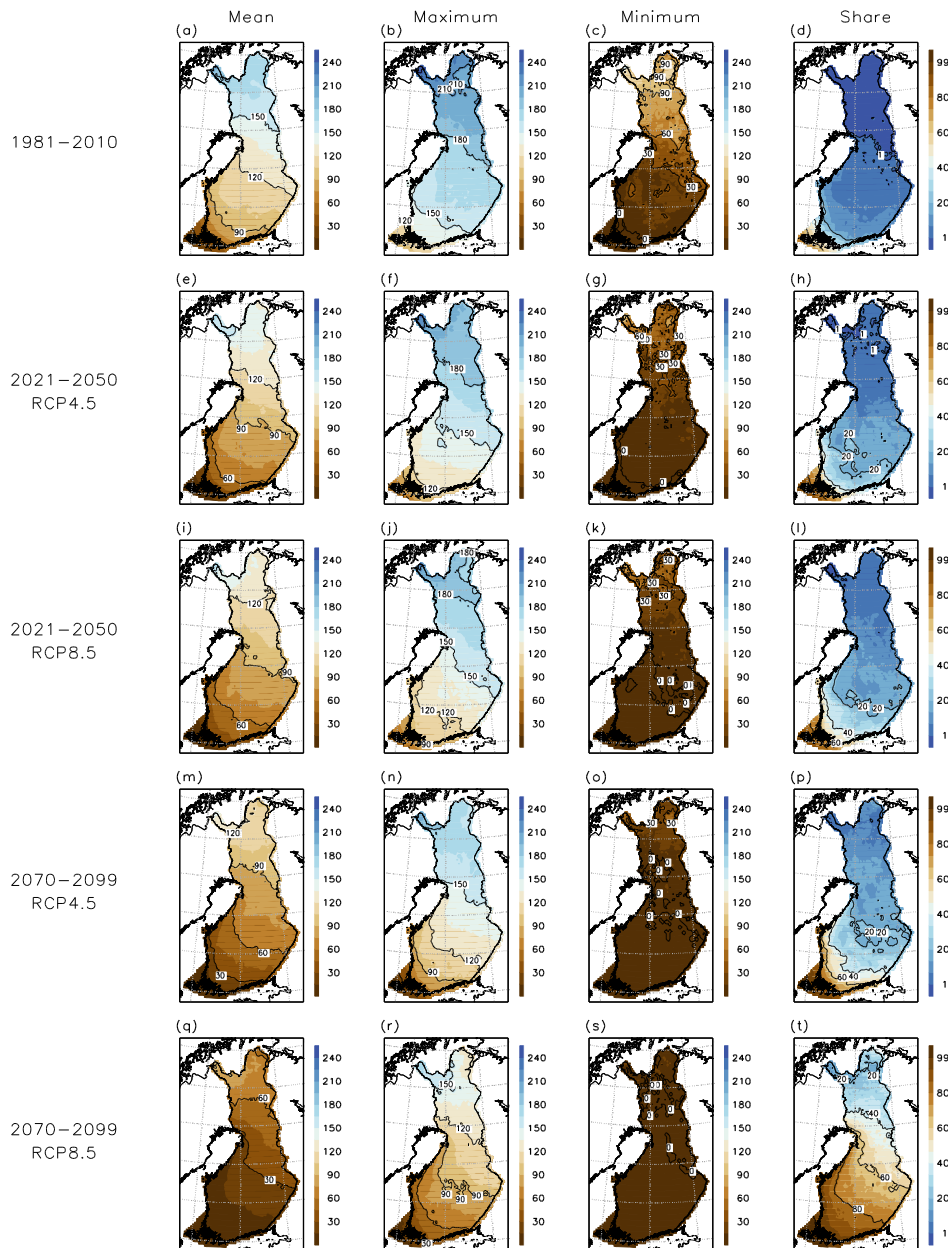


Figure 5. Modelled multi-GCM annual mean number of days with good bearing capacity in drained (pine dominated) peatlands during 1981–2010, 2021–2050 and 2070–2099 under the RCP4.5 and RCP8.5 scenarios (left panel). The second and third panel from the left show the modelled annual number of days with good bearing capacity during the winter with most (the second panel) and least (the third panel) such days within the 30-year periods based on the same multi-GCM mean. The last panel shows the share of winters (%) with less than 30 modelled days of good bearing capacity based on the multi-GCM mean.

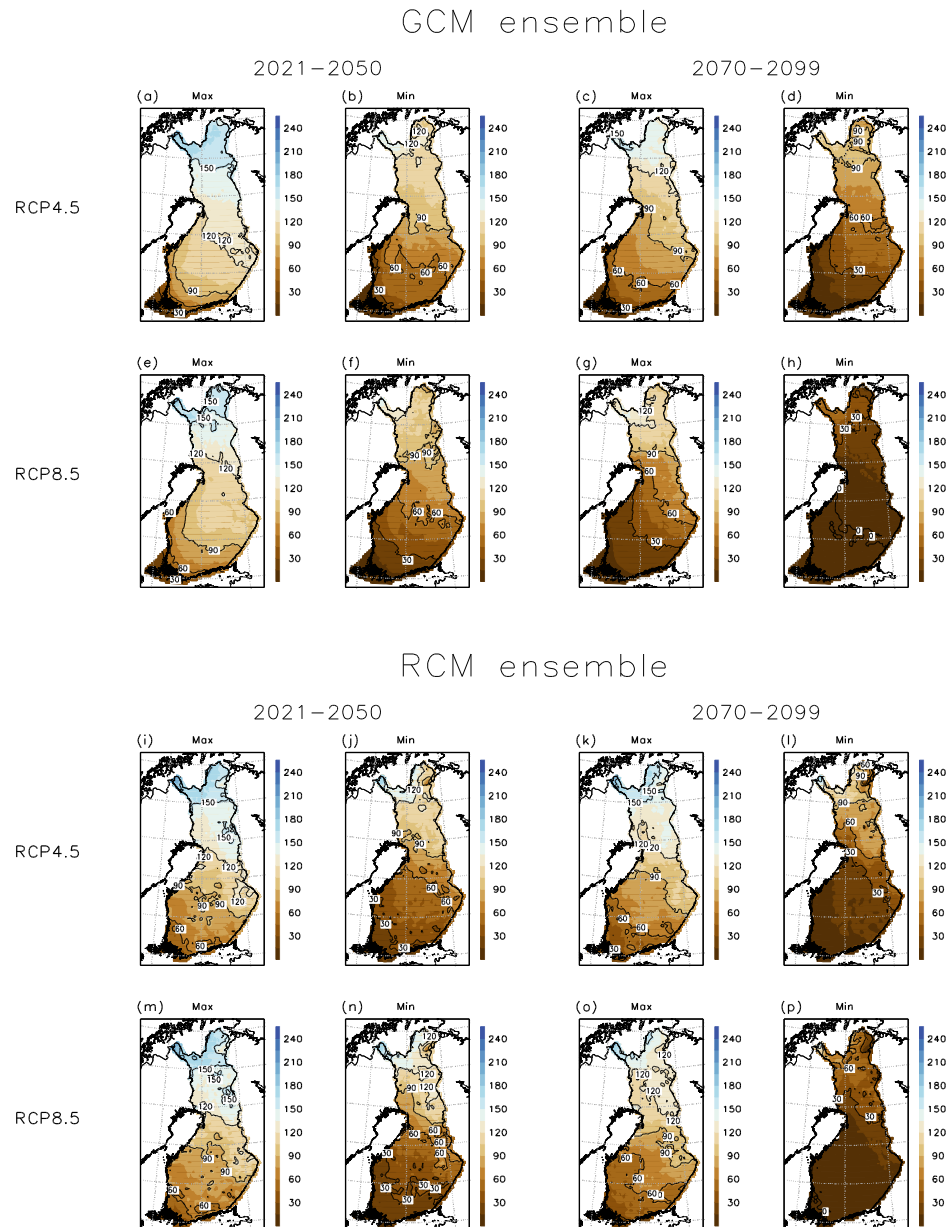


Figure 6. Range of modelled annual mean number of days with good bearing capacity in drained (pine dominated) peatlands during the periods 2021–2050 and 2070–2099 under the RCP4.5 and RCP8.5 scenarios among the GCMs and RCMs used in this study. The figures entitled with “Max” and “Min” show the highest and lowest modelled mean number of days with good bearing capacity among the used models for the GCMs and RCMs.